IASS-IACM 2012
GF Sarajevo, Bosnia and Herzegovina
Ibrahimbegovic, Dolarevic, Hrasnica
Madzarevic, Zlatar (eds.)

Geometrically exact structural models for large deformation problems in flexible multibody dynamics

P. Betsch[1], N. Sänger[1], C. Hesch[1]

[1] *University of Siegen, Paul-Bonatz-Straße 9–11, 57068 Siegen, Germany, betsch@imr.mb.uni-siegen.de, saenger@imr.mb.uni-siegen.de, hesch@imr.mb.uni-siegen.de*

Abstract — Computer methods for flexible multibody dynamics that are able to treat large deformation phenomena are important for specific applications such as contact problems. From a mechanical point of view, large deformation phenomena are formulated in the framework of nonlinear continuum mechanics. Computer methods for large deformation problems typically rely on the nonlinear finite element method. On the other hand classical formalisms for multibody dynamics are based on rigid bodies. Their extension to flexible multibody systems is typically restricted to linear elastic behavior. In the present work the nonlinear finite element method is extended such that the simulation of flexible multibody dynamics including large deformation phenomena can be handled successfully.
Key-words — Flexible multibody dynamics, geometrically exact beams and shells, natural coordinates, structure-preserving time integration, application of torques, large deformation contact.

1 Introduction

In the present work we address computer methods that can handle large deformations in the context of multibody systems. In particular, the link between nonlinear continuum mechanics and multibody systems is facilitated by a specific formulation of rigid body dynamics (Betsch & Steinmann [1]). This formulation is closely related to the notion of natural coordinates (García de Jalón [2]). Our approach makes possible the incorporation of state-of-the-art computer methods for large deformation problems. Examples are arbitrary constitutive models (Groß & Betsch [3]), geometrically exact beams (Ibrahimbegović & Mamouri [4]) and shells (Betsch & Sänger [5]), domain decomposition (Hesch & Betsch [6]), and large deformation contact (Hesch & Betsch [7]).

Energy and momentum consistent numerical methods for this kind of problems offer superior stability and robustness properties (Ibrahimbegović et al. [8]). Our approach relies on a uniform formulation of discrete mechanical systems such as rigid bodies and semi-discrete flexible bodies resulting from a finite element discretization of the underlying nonlinear continuum formulation. The uniform formulation results in discrete equations of motion assuming the form of differential-algebraic equations (DAEs). A constant inertia matrix is a characteristic feature of the present DAEs. In particular, the simple DAE structure makes possible the design of structure-preserving time-stepping schemes such as energy-momentum schemes and momentum-symplectic integrators (Leyendecker et al. [9], Betsch et al. [10]).

A further advantage of the present treatment of flexible and rigid bodies is that flexible multibody systems can be implemented in a very systematic way. In fact, the present approach leads to a generalization of the standard finite element assembly procedure. The generalized assembly procedure makes possible the incorporation of both arbitrary nonlinear finite element formulations and multibody features such as joints.

On the other hand the nonstandard description of rigid bodies requires some care concerning the consistent application of actuating forces. The present rigid body formulation falls into the framework of natural coordinates which have a long tradition in multibody system dynamics (see García de Jalón [2] and the references cited therein). By definition, natural coordinates are comprised of Cartesian components of unit vectors and Cartesian coordinates. It is worth noting that our specific choice of natural coordinates (Betsch & Steinmann [1]) has its roots in theoretical mechanics (Saletan & Cromer [11, Ch. 5]).

Using natural coordinates, the application of external torques becomes an issue since conjugate coordinates are not available. One way to resolve this issue is the introduction of additional coordinates which are appended to the natural coordinates via specific algebraic constraints, see, for example, García de Jalón [2] and Uhlar & Betsch [12]. Alternatively, the redundant forces conjugate to the natural coordinates can used to take into account the action of external torques. In the present work we focus on this approach. In particular, we show that the use of skew coordinates for the description of rigid body dynamics paves the way for the consistent time discretization of the equations of motion. The present approach has been guided by the close connection between natural coordinates and the theory of Cosserat points (Rubin [13]).

An outline of the rest of the paper is as follows. In Section 2 the equations of motion providing the framework for the present description of flexible multibody systems are summarized. The formulation of rigid body dynamics in terms of natural coordinates is dealt with in Section 3. The extension of the present approach to multibody dynamics is illustrated in Section 4 with the formulation of lower kinematic pairs. After a summary of the main features of the present approach in Section 5, the structure-preserving discretization in time is dealt with in Section 6. Section 7 comments on the inclusion of large deformation contact. To demonstrate the capability of the proposed method three numerical examples are presented in Section 8. Eventually, conclusions are drawn in Section 9.

2 Equations of motion

We start with the equations of motion pertaining to a finite-dimensional mechanical system subject to holonomic constraints. From the outset we confine ourselfs to mechanical systems whose kinetic energy can be written as

$$T(\dot{\boldsymbol{q}}) = \frac{1}{2}\dot{\boldsymbol{q}} \cdot \boldsymbol{M}\dot{\boldsymbol{q}} \tag{1}$$

Here, $\boldsymbol{q} \in \mathbb{R}^n$ is the vector of redundant coordinates and a superposed dot denotes the derivative with respect to time. Moreover $\boldsymbol{M} \in \mathbb{R}^{n\times n}$ is a **constant** mass matrix. As has been outlined in the Introduction a constant mass matrix is a consequence of the use of natural coordinates for the description of spatial multibody systems. The equations of motion pertaining to the discrete mechanical systems of interest can be written in variational form

$$G^{\delta} = \delta\boldsymbol{q} \cdot \left(\boldsymbol{M}\ddot{\boldsymbol{q}} + \sum_{l=1}^{m} \lambda^{l} \nabla g_l(\boldsymbol{q}) - \boldsymbol{F}\right) = 0 \tag{2}$$

which has to be satisfied for arbitrary $\delta\boldsymbol{q} \in \mathbb{R}^n$. The last equation has to be supplemented with algebraic constraint equations $g_l(\boldsymbol{q}) = 0$, $1 \leq l \leq m$. The associated constraint forces assume the form $\sum \lambda^l \nabla g_l(\boldsymbol{q})$, where λ^l are Lagrange multipliers. The last term in (2) accounts for external forcing. For simplicity of exposition we do not distinguish between forces that can be derived from potentials and nonpotential forces. Note, however, that we may replace $\boldsymbol{F} \in \mathbb{R}^n$ in (2) with

$$\boldsymbol{F} \to \boldsymbol{F} - \nabla U(\boldsymbol{q}) \tag{3}$$

Then, the potential forces are derived from a potential function $U(\boldsymbol{q})$, and the nonpotential forces are contained in $\boldsymbol{F}$. Due to the presence of algebraic constraints the equations of motion assume the form of differential-algebraic equations (*DAEs*). The configuration space of the constrained mechanical systems under consideration is defined by

$$\mathsf{Q} = \{\boldsymbol{q} \in \mathbb{R}^n | g_l(\boldsymbol{q}) = 0\,,\ 1 \leq l \leq m\} \tag{4}$$

Throughout this work we assume that the constraints are independent. Consequently, the vectors $\nabla g_l(\boldsymbol{q}) \in \mathbb{R}^n$ are linearly independent for $\boldsymbol{q} \in \mathsf{Q}$. Due to the presence of m geometric constraints the discrete mechanical system under consideration has $n - m$ degrees of freedom. Admissible variations $\delta\boldsymbol{q}$ have to belong to the tangent space to Q at $\boldsymbol{q} \in \mathsf{Q}$ given by

$$T_q\mathsf{Q} = \{\boldsymbol{v} \in \mathbb{R}^n | \nabla g_l(\boldsymbol{q}) \cdot \boldsymbol{v} = 0\,,\ 1 \leq l \leq m\} \tag{5}$$

Remark 2.1 *The variational form (2) of the equations of motion is equivalent to Lagrange's equations (of the first kind), which may be linked to the Lagrange-d'Alembert principle*

$$\delta \int_{t_0}^{t_N} \left(T(\dot{\boldsymbol{q}}) - \sum_{l=1}^{m} \lambda^l g_l(\boldsymbol{q}) \right) dt + \int_{t_0}^{t_N} \delta \boldsymbol{q} \cdot \boldsymbol{F}\, dt = 0 \tag{6}$$

The Lagrange-d'Alembert principle can be viewed as an extension of Hamilton's principle to account for external forcing, see Marsden & Ratiu [14].

Remark 2.2 *In the above description $\boldsymbol{F} \in \mathbb{R}^n$ is loosely termed 'external force vector'. In a multibody system formulated in terms of natural coordinates each individual component of $\boldsymbol{F}$ refers to a specific rigid body (see Section 3 for further details) or a specific node of the finite element discretization of a flexible beam or shell component. Thus the action of joint-forces can be respresented by components of $\boldsymbol{F}$, although joint-forces are internal forces (or torques) from the multibody system perspective. If the external force components are to represent joint-forces Newton's third (or action-reaction) law has to be obeyed.*

3 Rigid body dynamics in terms of skew coordinates

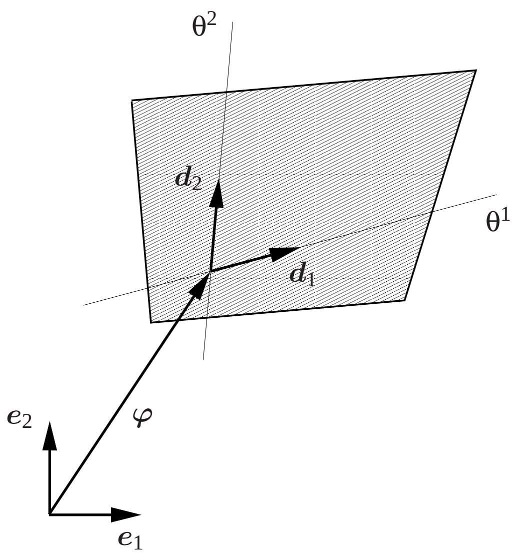

Figure 1: Planar sketch of the rigid body.

We next present a reformulation of the original formulation of rigid body dynamics (Betsch & Steinmann [1]) and Saletan & Cromer [11, Ch. 5]) in terms of skew coordinates. The use of skew coordinates turns out to be beneficial to the formulation and consistent numerical discretization of external torques. In the following we use convected coordinates θ^i to label a material point belonging to the rigid body (Fig. 1). The position of a material point at time t can be described by

$$\boldsymbol{x} = \boldsymbol{\chi}(\theta^i, t) = \boldsymbol{\varphi}(t) + \theta^i \boldsymbol{d}_i(t) \tag{7}$$

where $\boldsymbol{\varphi} = \varphi_i \boldsymbol{e}_i$ is a reference point fixed in the body and $\boldsymbol{d}_i = (d_i)_j \boldsymbol{e}_j$ are director vectors[1]. Due to the kinematic relation (7), the covariant base vectors coincide with the directors, i.e. $\boldsymbol{g}_i = \partial \boldsymbol{x} / \partial \theta^i = \boldsymbol{d}_i$. For the time being the directors $\boldsymbol{d}_i$ can be regarded as base vectors that need not be of unit length nor mutually orthogonal. As mentioned before, the present use of skew coordinates can be viewed as generalization of previous rigid body formulations relying on the components of the direction-cosine matrix (see Saletan

[1]Note that the summation convention applies to lower case roman indices occuring twice in a term. They generally range from one to three.

& Cromer [11, Ch. 5] and Betsch & Steinmann [1]). This generalization turns out to be advantageous for the discretization in time dealt with in Section 6. We further assume

$$d^{\frac{1}{2}} = \boldsymbol{d}_1 \cdot (\boldsymbol{d}_2 \times \boldsymbol{d}_3) > 0 \tag{8}$$

Additional constraints will be imposed in the sequel to enforce the rigid body assumption. In addition to the covariant base vectors we introduce contravariant base vectors

$$\boldsymbol{d}^i = d^{-\frac{1}{2}} (\boldsymbol{d}_j \times \boldsymbol{d}_k) \tag{9}$$

for even permutations of the indices (i, j, k). Consequently, $\boldsymbol{d}^i \cdot \boldsymbol{d}_j = \delta^i_j$, the Kronecker delta. In the following the contravariant base vectors $\boldsymbol{d}^i$ will be called covariant directors.

The kinematic relationship (7) indicates that the configuration of a single rigid body can be described by $n = 12$ coordinates that can be arranged in the configuration vector

$$\boldsymbol{q} = \begin{bmatrix} \boldsymbol{\varphi} \\ \boldsymbol{d}_1 \\ \boldsymbol{d}_2 \\ \boldsymbol{d}_3 \end{bmatrix} \tag{10}$$

To calculate the mass matrix $\boldsymbol{M} \in \mathbb{R}^{12\times 12}$ we consider the continuum expression for the kinetic energy

$$T = \frac{1}{2} \int_{\mathcal{B}_0} \rho_0 \boldsymbol{v} \cdot \boldsymbol{v} D^{\frac{1}{2}} d^3\theta \tag{11}$$

where $\mathcal{B}_0$ denotes the reference configuration of the body at time $t = 0$. Correspondingly, $\rho_0 : \mathcal{B}_0 \to \mathbb{R}_+$ is the reference mass density and $D = d(0)$, where $d(t)$ is given by (8). The material velocity $\boldsymbol{v}$ can be calculated from (7):

$$\boldsymbol{v} = \frac{\partial}{\partial t} \boldsymbol{\chi}(\theta^i, t) = \boldsymbol{v}_\varphi(t) + \theta^i \boldsymbol{v}_i(t) \tag{12}$$

Here $\boldsymbol{v}_\varphi = \dot{\boldsymbol{\varphi}}$ is the velocity of the point of reference and $\boldsymbol{v}_i = \dot{\boldsymbol{d}}_i$ will be referred to as director velocities. Inserting the last equation into (11) a straightforward calculation yields the kinetic energy in the form

$$T = \frac{1}{2} M_\varphi \boldsymbol{v}_\varphi \cdot \boldsymbol{v}_\varphi + e^i \boldsymbol{v}_\varphi \cdot \boldsymbol{v}_i + \frac{1}{2} E^{ij} \boldsymbol{v}_i \cdot \boldsymbol{v}_j \tag{13}$$

In the last equation the total mass M_φ and the director inertia coefficients e^i, E^{ij} are defined by

$$M_\varphi = \int_{\mathcal{B}_0} \rho_0 D^{\frac{1}{2}} d^3\theta, \qquad e^i = \int_{\mathcal{B}_0} \theta^i \rho_0 D^{\frac{1}{2}} d^3\theta, \qquad E^{ij} = \int_{\mathcal{B}_0} \theta^i \theta^j \rho_0 D^{\frac{1}{2}} d^3\theta \tag{14}$$

Note that that all of the inertia coefficients are independent of time thus leading to a constant 12×12 mass matrix given by

$$\boldsymbol{M} = \begin{bmatrix} M_\varphi \boldsymbol{I} & e^1 \boldsymbol{I} & e^2 \boldsymbol{I} & e^3 \boldsymbol{I} \\ e^1 \boldsymbol{I} & E^{11} \boldsymbol{I} & E^{12} \boldsymbol{I} & E^{13} \boldsymbol{I} \\ e^2 \boldsymbol{I} & E^{21} \boldsymbol{I} & E^{22} \boldsymbol{I} & E^{23} \boldsymbol{I} \\ e^3 \boldsymbol{I} & E^{31} \boldsymbol{I} & E^{32} \boldsymbol{I} & E^{33} \boldsymbol{I} \end{bmatrix} \tag{15}$$

To determine the external force vector $\boldsymbol{F}$ in (2), we consider the virtual work of the external forces given by $\delta W = \delta \boldsymbol{q} \cdot \boldsymbol{F}$. For simplicity we assume that in addition to a body force per unit mass, $\boldsymbol{b}(\theta^i, t)$, a single force vector $\boldsymbol{f}(t)$ is applied to the material point Θ^i. Accordingly,

$$\delta W = \int_{\mathcal{B}_0} \delta x \cdot \boldsymbol{b} \rho_0 D^{\frac{1}{2}} d^3\theta + \delta x(\Theta^i) \cdot \boldsymbol{f}(t) \tag{16}$$

With regard to (7), virtual displacements can be written as $\delta \boldsymbol{x} = \delta \boldsymbol{\varphi} + \theta^i \delta \boldsymbol{d}_i$. Accordingly, (16) gives rise to

$$\delta W = \delta \boldsymbol{\varphi} \cdot \boldsymbol{f}_\varphi + \delta \boldsymbol{d}_i \cdot \boldsymbol{f}^i \tag{17}$$

where the resultant force vector is given by

$$\boldsymbol{f}_\varphi = \int_{\mathcal{B}_0} \boldsymbol{b}\rho_0 D^{\frac{1}{2}} d^3\theta + \boldsymbol{f} \tag{18}$$

and the resultant director forces assume the form

$$\boldsymbol{f}^i = \int_{\mathcal{B}_0} \theta^i \boldsymbol{b}\rho_0 D^{\frac{1}{2}} d^3\theta + \Theta^i \boldsymbol{f} \tag{19}$$

Note that the resultant force vector $\boldsymbol{f}_\varphi$ and the resultant director forces $\boldsymbol{f}^i$ are conjugate to $\boldsymbol{\varphi}$ and the directors $\boldsymbol{d}_i$. Similar to the configuration vector (10) of the rigid body, the vector of the external forces featuring in the equations of motion (2) can be written as

$$\boldsymbol{F} = \begin{bmatrix} \boldsymbol{f}_\varphi \\ \boldsymbol{f}^1 \\ \boldsymbol{f}^2 \\ \boldsymbol{f}^3 \end{bmatrix} \tag{20}$$

The equations of motion pertaining to the rigid body can now be written in the variational form

$$\begin{aligned} \delta\boldsymbol{\varphi} \cdot \left\{ M_\varphi \dot{\boldsymbol{v}}_\varphi + e^i \dot{\boldsymbol{v}}_i + \boldsymbol{f}_c - \boldsymbol{f}_\varphi \right\} &= 0 \\ \delta\boldsymbol{d}_i \cdot \left\{ E^{ij} \dot{\boldsymbol{v}}_j + e^i \dot{\boldsymbol{v}}_\varphi + \boldsymbol{f}_c^i - \boldsymbol{f}^i \right\} &= 0 \end{aligned} \tag{21}$$

Here, $\boldsymbol{f}_c$ and $\boldsymbol{f}_c^i$ stand for the constraint forces and the constraint director forces, respectively. For the free rigid body, $\boldsymbol{f}_c = \boldsymbol{0}$. The specific form of the constraint director forces will be dealt with in the sequel.

3.1 Rigid body constraints

The rigid body assumption can be incorporated into the present formulation by excluding deformation of the director triad $\{\boldsymbol{d}_i\}$. This goal can be achieved by providing the following six constraint functions

$$\begin{aligned} &g_1 = \tfrac{1}{2}(\boldsymbol{d}_1 \cdot \boldsymbol{d}_1 - c_1) \qquad && g_2 = \tfrac{1}{2}(\boldsymbol{d}_2 \cdot \boldsymbol{d}_2 - c_2) \qquad && g_3 = \tfrac{1}{2}(\boldsymbol{d}_3 \cdot \boldsymbol{d}_3 - c_3) \\ &g_4 = \boldsymbol{d}_1 \cdot \boldsymbol{d}_2 - c_4 && g_5 = \boldsymbol{d}_1 \cdot \boldsymbol{d}_3 - c_5 && g_6 = \boldsymbol{d}_2 \cdot \boldsymbol{d}_3 - c_6 \end{aligned} \tag{22}$$

where c_i $(i = 1, \ldots, 6)$ are constant parameters to be specified in the reference configuration. The corresponding constraint equations $g_i = 0$ have to be satisfied at all times. With regard to (4), the six independent constraints (22) determine the configuration manifold Q^{free} of the free rigid body. It is worth mentioning that the associated tangent space (5) is given by

$$T_q\mathsf{Q}^{\text{free}} = \{\boldsymbol{v}_\varphi \in \mathbb{R}^3, \boldsymbol{v}_i \in \mathbb{R}^3\,(i = 1,2,3)\,|\,\boldsymbol{v}_i = \boldsymbol{\omega} \times \boldsymbol{d}_i, \boldsymbol{\omega} \in \mathbb{R}^3\} \tag{23}$$

where $\boldsymbol{\omega} \in \mathbb{R}^3$ can be interpreted as angular velocity.

3.2 Balance laws

Next we elaborate on the fundamental mechanical balance laws in the context of the free rigid body. First, we consider the **balance law for linear momentum**. Introducing $\delta\boldsymbol{\varphi} = \boldsymbol{\xi}$, where $\boldsymbol{\xi} \in \mathbb{R}^3$ is a constant vector, together with $\delta\boldsymbol{d}_i = \boldsymbol{0}$ into (21), a straigthforward calculation gives

$$\frac{d}{dt}\boldsymbol{L} = \boldsymbol{f}_\varphi \tag{24}$$

Here, the total linear momentum of the rigid body is given by $\boldsymbol{L} = M_\varphi \boldsymbol{v}_\varphi + e^i \boldsymbol{v}_i$, and, as before, the right-hand side of (24) characterizes the resultant external force applied to the rigid body.

Concerning the **balance law for angular momentum**, substitute $\delta\boldsymbol{\varphi} = \boldsymbol{\xi} \times \boldsymbol{\varphi}$ along with $\delta\boldsymbol{d}_i = \boldsymbol{\xi} \times \boldsymbol{d}_i$ into (21) and subsequently take the sum of both equations. This procedure yields

$$\boldsymbol{\xi} \cdot \left[\boldsymbol{\varphi} \times \{ M_\varphi \dot{\boldsymbol{v}}_\varphi + e^i \dot{\boldsymbol{v}}_i - \boldsymbol{f}_\varphi \} + \boldsymbol{d}_i \times \{ E^{ij} \dot{\boldsymbol{v}}_j + e^i \dot{\boldsymbol{v}}_\varphi + \boldsymbol{f}_c^i - \boldsymbol{f}^i \} \right] = 0 \tag{25}$$

Since for the free rigid body (21) has to hold for arbitary $\delta\boldsymbol{\varphi} \in \mathbb{R}^3$ and $\delta\boldsymbol{d}_i \in \mathbb{R}^3$ $(i = 1,2,3)$, the last equation yields the reduced form of the balance of angular momentum

$$\boldsymbol{d}_i \times \boldsymbol{f}_c^i = \boldsymbol{0} \tag{26}$$

This condition places three restrictions on the constraint director forces $\boldsymbol{f}_c^i$. Expressing the constraint director forces with respect to the director basis

$$\boldsymbol{f}_c^i = \Lambda^{ij}\boldsymbol{d}_j \tag{27}$$

condition (26) yields $\Lambda^{ij}\boldsymbol{d}_i \times \boldsymbol{d}_j = \boldsymbol{0}$. Due to the skew-symmetriy of the cross product, we get the symmetry property $\Lambda^{ij} = \Lambda^{ji}$. Accordingly, there remain only six indpendent components Λ^{ij} for the specification of the constraint director forces. In particular, the six independent constraints (22) of rigidity yield constraint director forces of the form

$$\boldsymbol{f}_c^i = \sum_{l=1}^{6} \lambda^l \nabla_{\boldsymbol{d}_i} g_l \tag{28}$$

Combining (27) and (28), the components Λ^{ij} can be connected to the Lagrange multipliers:

$$[\Lambda^{ij}] = \begin{bmatrix} \lambda^1 & \lambda^4 & \lambda^5 \\ \lambda^4 & \lambda^2 & \lambda^6 \\ \lambda^5 & \lambda^6 & \lambda^3 \end{bmatrix} \tag{29}$$

Returning to (25) and taking into account (26), we further get

$$\boldsymbol{\xi} \cdot \left[\boldsymbol{\varphi} \times \frac{d}{dt}\{M_\varphi \boldsymbol{v}_\varphi + e^i \boldsymbol{v}_i\} + \boldsymbol{d}_i \times \frac{d}{dt}\{E^{ij}\boldsymbol{v}_j + e^i \boldsymbol{v}_\varphi\} - \{\boldsymbol{\varphi} \times \boldsymbol{f}_\varphi + \boldsymbol{d}_i \times \boldsymbol{f}^i\} \right] = 0 \tag{30}$$

The last equation can be recast in the form

$$\frac{d}{dt}\boldsymbol{J} = \boldsymbol{\varphi} \times \boldsymbol{f}_\varphi + \boldsymbol{d}_i \times \boldsymbol{f}^i \tag{31}$$

where

$$\boldsymbol{J} = \boldsymbol{\varphi} \times \{M_\varphi \boldsymbol{v}_\varphi + e^i \boldsymbol{v}_i\} + \boldsymbol{d}_i \times \{E^{ij}\boldsymbol{v}_j + e^i \boldsymbol{v}_\varphi\} \tag{32}$$

is the total angular momentum of the rigid body with respect to the origin of the inertial frame of reference. The right-hand side of (31) equals the resultant external torque about the origin. Note that

$$\boldsymbol{d}_i \times \boldsymbol{f}^i = \boldsymbol{m} \tag{33}$$

can be identified as the resultant external torque relative to the point of reference of the rigid body.

We eventually turn to the **balance of energy**. Substituting $\boldsymbol{v}_\varphi$ for $\delta\boldsymbol{\varphi}$ and $\boldsymbol{v}_i$ for $\delta\boldsymbol{d}_i$, (21) leads to

$$\begin{aligned} \boldsymbol{v}_\varphi \cdot \left\{M_\varphi \dot{\boldsymbol{v}}_\varphi + e^i \dot{\boldsymbol{v}}_i\right\} &= \boldsymbol{f}_\varphi \cdot \boldsymbol{v}_\varphi \\ \boldsymbol{v}_i \cdot \left\{E^{ij}\dot{\boldsymbol{v}}_j + e^i \dot{\boldsymbol{v}}_\varphi\right\} &= \boldsymbol{f}^i \cdot \boldsymbol{v}_i - \boldsymbol{f}_c^i \cdot \boldsymbol{v}_i \end{aligned} \tag{34}$$

Note that the director velocities have to belong to the tangent space (23). This implies the relationship $\boldsymbol{v}_i = \boldsymbol{\omega} \times \boldsymbol{d}_i$, where $\boldsymbol{\omega} \in \mathbb{R}^3$ is the angular velocity. Accordingly,

$$\boldsymbol{f}_c^i \cdot \boldsymbol{v}_i = \boldsymbol{f}_c^i \cdot (\boldsymbol{\omega} \times \boldsymbol{d}_i) = \boldsymbol{\omega} \cdot (\boldsymbol{d}_i \times \boldsymbol{f}_c^i) = \boldsymbol{0} \tag{35}$$

where condition (26) has been used. The last equation conveys the well-known fact that constraint forces are workless. Taking the sum of both equations in (34) yields the balance of energy

$$\frac{d}{dt}T = P^{\text{ext}} \tag{36}$$

where

$$P^{\text{ext}} = \boldsymbol{f}_\varphi \cdot \boldsymbol{v}_\varphi + \boldsymbol{f}^i \cdot \boldsymbol{v}_i \tag{37}$$

denotes the power of the external forces acting on the rigid body. It is worth noting that the last equation can also be written in the form

$$P^{\text{ext}} = \boldsymbol{f}_\varphi \cdot \boldsymbol{v}_\varphi + \boldsymbol{m} \cdot \boldsymbol{\omega} \tag{38}$$

where the relationship $\boldsymbol{v}_i = \boldsymbol{\omega} \times \boldsymbol{d}_i$ along with definition (33) of the resultant external torque relative to the point of reference of the rigid body have been used.

3.3 Application of external torques

It can be concluded from (38) that the resultant external torque $\boldsymbol{m}$ is conjugate to the angular velocity $\boldsymbol{\omega}$. In contrast to that, the formulation in terms of natural coordinates relies on the resultant external director forces $\boldsymbol{f}^i$ which are conjugate to the director velocities $\boldsymbol{v}_i$, see (37). Using natural coordinates the question arises how the application of external torques can be realized. To answer this question we start with the kinematic relationship $\boldsymbol{v}_i = \boldsymbol{\omega} \times \boldsymbol{d}_i$ and calculate

$$\begin{aligned} \boldsymbol{d}^i \times \boldsymbol{v}_i &= \boldsymbol{d}^i \times (\boldsymbol{\omega} \times \boldsymbol{d}_i) \\ &= \left\{ (\boldsymbol{d}^i \cdot \boldsymbol{d}_i)\boldsymbol{I} - \boldsymbol{d}_i \otimes \boldsymbol{d}^i \right\} \boldsymbol{\omega} \\ &= 2\boldsymbol{\omega} \end{aligned} \tag{39}$$

Using this result, the work done by the external torque $\boldsymbol{m}$ can be written as

$$\begin{aligned} \boldsymbol{m} \cdot \boldsymbol{\omega} &= \frac{1}{2}\boldsymbol{m} \cdot (\boldsymbol{d}^i \times \boldsymbol{v}_i) \\ &= \frac{1}{2}\boldsymbol{v}_i \cdot (\boldsymbol{m} \times \boldsymbol{d}^i) \end{aligned} \tag{40}$$

Since, with regard to (37), the corresponding work expression in terms of natural coordinates is given by $\boldsymbol{v}_i \cdot \boldsymbol{f}^i$, the external director forces assume the form

$$\boldsymbol{f}^i = \frac{1}{2}\boldsymbol{m} \times \boldsymbol{d}^i \tag{41}$$

This expression can be used to realize the application of an external torque $\boldsymbol{m}$.

4 Kinematic pairs in terms of natural coordinates

We next illustrate the formulation of kinematic pairs with the example of a cylindrical pair (Fig. 2). To this end we consider two rigid bodies formulated in terms of natural coordinates as outlined in Section 3. Accordingly, the configuration of the two-body system under consideration is characterized by redundant coordinates

$$\boldsymbol{q} = \begin{bmatrix} {}^1\boldsymbol{q} \\ {}^2\boldsymbol{q} \end{bmatrix} \quad \text{where} \quad {}^\alpha\boldsymbol{q} = \begin{bmatrix} {}^\alpha\boldsymbol{\varphi} \\ {}^\alpha\boldsymbol{d}_1 \\ {}^\alpha\boldsymbol{d}_2 \\ {}^\alpha\boldsymbol{d}_3 \end{bmatrix} \tag{42}$$

Note that the contribution of body α to the configuration vector coincides with (10). The equations of motion pertaining to the constrained mechanical system at hand can again be formulated as outlined in Section 2. Similar to (42), the contribution of each rigid body to the external forces leads to the system vector

$$\boldsymbol{F} = \begin{bmatrix} {}^1\boldsymbol{F} \\ {}^2\boldsymbol{F} \end{bmatrix} \quad \text{where} \quad {}^\alpha\boldsymbol{F} = \begin{bmatrix} {}^\alpha\boldsymbol{f}_\varphi \\ {}^\alpha\boldsymbol{f}^1 \\ {}^\alpha\boldsymbol{f}^2 \\ {}^\alpha\boldsymbol{f}^3 \end{bmatrix} \tag{43}$$

Note that the force vector ${}^\alpha\boldsymbol{F}$ associated with body α coincides with (10).

4.1 Initialization of kinematic relationships

To describe the motion of the second body relative to the first one we introduce orthonormal body-fixed triads $\{{}^\alpha\boldsymbol{d}'_i\}$ in such a way that the unit vectors ${}^\alpha\boldsymbol{d}'_3$ are parallel to the axis of the cylindrical pair (Fig. 2). Moreover, we choose the two orthonormal triads to coincide in the initial configuration, i.e. ${}^1\boldsymbol{d}'_i(0) = {}^2\boldsymbol{d}'_i(0)$. The connection between the newly introduced orthonormal triads $\{{}^\alpha\boldsymbol{d}'_i\}$ and the original triads $\{{}^\alpha\boldsymbol{d}_i\}$ (i.e. the natural coordinates) is given by

$${}^\alpha\boldsymbol{R}' = {}^\alpha\boldsymbol{F}\,{}^\alpha\boldsymbol{\Lambda}_0 \tag{44}$$

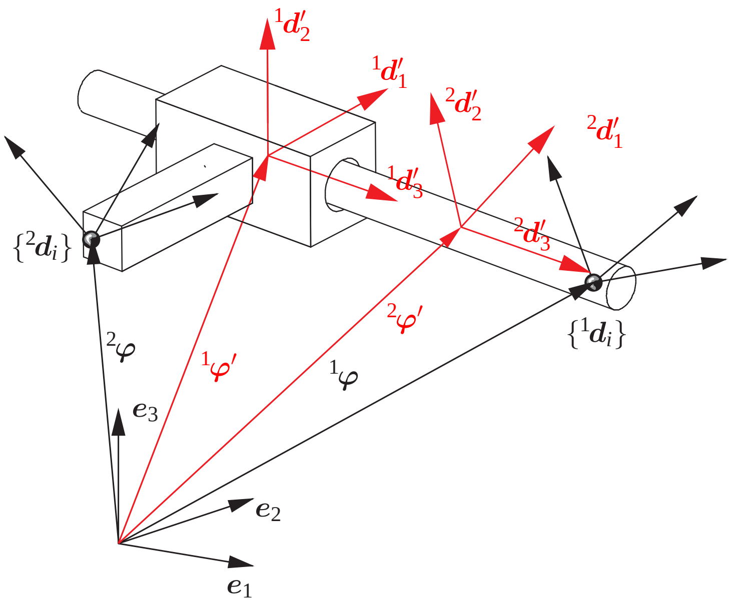

Figure 2: Sketch of the cylindrical pair: Natural coordinates $({}^\alpha\boldsymbol{\varphi}, \{{}^\alpha\boldsymbol{d}_i\})$ characterizing the current configuration ${}^\alpha\mathcal{B}_t$ of rigid body α. The additional systems $({}^\alpha\boldsymbol{\varphi}', \{{}^\alpha\boldsymbol{d}'_i\})$ are introduced for the description of the motion of the second body relative to the first body (translation along and rotation about ${}^1\boldsymbol{d}'_3 = {}^2\boldsymbol{d}'_3$). The connection between $({}^\alpha\boldsymbol{\varphi}', \{{}^\alpha\boldsymbol{d}'_i\})$ and the natural coordinates $({}^\alpha\boldsymbol{\varphi}, \{{}^\alpha\boldsymbol{d}_i\})$ is defined in the initial configuration of the multibody system.

where

$$ {}^\alpha\boldsymbol{F} = {}^\alpha\boldsymbol{d}_i \otimes \boldsymbol{e}^i \quad \text{and} \quad {}^\alpha\boldsymbol{R}' = {}^\alpha\boldsymbol{d}'_i \otimes \boldsymbol{e}^i \tag{45} $$

The constant tensors ${}^\alpha\boldsymbol{\Lambda}_0$ in (44) are calculated in the initial configuration via

$$ {}^\alpha\boldsymbol{\Lambda}_0 = {}^\alpha\boldsymbol{F}^{-1}(0)\,{}^\alpha\boldsymbol{R}'(0) \tag{46} $$

The origin of the newly introduced orthonormal triads $\{{}^\alpha\boldsymbol{d}'_i\}$ is fixed at material points ${}^\alpha\Theta^i$ whose placement in the current configuration ${}^\alpha\mathcal{B}_t$ of rigid body α is denoted by ${}^\alpha\boldsymbol{\varphi}'$. Accordingly, making use of the rigid body kinematics (7),

$$ {}^\alpha\boldsymbol{\varphi}' = {}^\alpha\boldsymbol{\varphi} + {}^\alpha\Theta^i\,{}^\alpha\boldsymbol{d}_i \tag{47} $$

Note that the location of the material points ${}^\alpha\Theta^i$ has to be specified during initialization.

4.2 Configuration space of the cylindrical pair

The configuration space of the cylindrical pair can be easily defined by distinguishing between internal constraints due the assumption of rigidity and external constraints due to the interconnection between the rigid bodies in a multibody system (see Betsch & Steinmann [15]). Accordingly, the present description of the cylindrical pair relies on $n = 24$ natural coordinates subject to 12 internal constraints $\boldsymbol{g}^{\text{int}}({}^\alpha\boldsymbol{q}) = \boldsymbol{0}$ $(\alpha = 1, 2)$, where $\boldsymbol{g}^{\text{int}} : \mathbb{R}^{12} \to \mathbb{R}^6$ follows from (22), and 4 external constraints associated with the constraint functions

$$ \boldsymbol{g}^{\text{ext}}_{\text{P}}(\boldsymbol{q}) = \begin{bmatrix} {}^1\boldsymbol{d}'_1 \cdot ({}^2\boldsymbol{\varphi}' - {}^1\boldsymbol{\varphi}') \\ {}^1\boldsymbol{d}'_2 \cdot ({}^2\boldsymbol{\varphi}' - {}^1\boldsymbol{\varphi}') \end{bmatrix} \tag{48} $$

and

$$ \boldsymbol{g}^{\text{ext}}_{\text{R}}(\boldsymbol{q}) = \begin{bmatrix} {}^1\boldsymbol{d}'_1 \cdot {}^2\boldsymbol{d}'_3 \\ {}^1\boldsymbol{d}'_2 \cdot {}^2\boldsymbol{d}'_3 \end{bmatrix} \tag{49} $$

To summarize, we have $n = 24$ coordinates subject to $m = 16$ constraints which can be assembled in the constraint function $\boldsymbol{g}^{\text{C}} : \mathbb{R}^{24} \to \mathbb{R}^{16}$ given by

$$ \boldsymbol{g}^{\text{C}}(\boldsymbol{q}) = \begin{bmatrix} \boldsymbol{g}^{\text{int}}({}^1\boldsymbol{q}) \\ \boldsymbol{g}^{\text{int}}({}^2\boldsymbol{q}) \\ \boldsymbol{g}^{\text{ext}}_{\text{P}}(\boldsymbol{q}) \\ \boldsymbol{g}^{\text{ext}}_{\text{R}}(\boldsymbol{q}) \end{bmatrix} \tag{50} $$

Consequently, the configuration space of the cylindrical pair is defined by

$$\mathsf{Q}^{\mathrm{C}} = \{\boldsymbol{q} \in \mathbb{R}^{24} \,|\, \boldsymbol{g}^{\mathrm{C}}(\boldsymbol{q}) = \boldsymbol{0}\} \tag{51}$$

5 Main features of natural coordinates

Before we deal with the discretization in time we summarize main features of the formulation of flexible multibody dynamics in terms of natural coordinates. In this connection it is important to note that geometrically exact models for beams and shells fit perfectly well into the present framework. In partiucular, if the nonlinear beam and shell formulations are discretized in space as proposed by Betsch et al. [16, 17, 5], the equations of motion pertaining to the resulting discrete mechanical systems fit into the framework outlined in Section 2. Thus the use of natural coordinates makes possible a uniform formulation of flexible multibody dynamics[2]. Main characteristics of the present approach can be summarized as follows:

1. The inertia parameters are always constant leading to the simple structure of the inertia terms in the equations of motion (see Section 2). In particular, the differential part of the equations of motion can be written as
$$\boldsymbol{M}\ddot{\boldsymbol{q}} + \nabla V_{\lambda}(\boldsymbol{q}) - \boldsymbol{F} = \boldsymbol{0} \tag{52}$$
where the potential forces along with the constraint forces can be derived from an augmented potential function of the form
$$V_{\lambda}(\boldsymbol{q}) = U(\boldsymbol{q}) + \sum_{l=1}^{m} \lambda^l \nabla g_l(\boldsymbol{q}) \tag{53}$$
For example, the potential function $U(\boldsymbol{q})$ can be associated with the action of gravitational forces or with the deformation of elastic components such as flexible beams and shells.

2. The configuration vector of the complete flexible multibody system is composed of vectors $\boldsymbol{q}_I \in \mathbb{R}^3$ and thus given by
$$\boldsymbol{q} = \begin{bmatrix} \boldsymbol{q}_1 \\ \boldsymbol{q}_2 \\ \vdots \\ \boldsymbol{q}_{\mathcal{N}} \end{bmatrix} \tag{54}$$
Accordingly, in total, the configuration vector $\boldsymbol{q} \in \mathbb{R}^n$ has $n = 3\mathcal{N}$ components.

3. The total angular momentum of the flexible multibody systems can be cast in the form
$$\boldsymbol{J} = \sum_{a,b=1}^{\mathcal{N}} M^{ab} \boldsymbol{q}_a \times \boldsymbol{v}_b \tag{55}$$
where M^{ab} contain the constant inertia parameters and $\boldsymbol{v}_b = \dot{\boldsymbol{q}}_b$.

4. The balance of angular momentum can be written as
$$\frac{d}{dt}\boldsymbol{J} = \sum_{a=1}^{\mathcal{N}} \boldsymbol{q}_a \times (\boldsymbol{F}^a - \nabla_{\boldsymbol{q}_a} V_{\lambda}(\boldsymbol{q})) \tag{56}$$

Needless to say that these features have a strong impact on the discretization in time.

[2] The present framework comprises as well domain decomposition problems (see Hesch & Betsch [6]) and large deformation contact (see Hesch & Betsch [7, 18, 19])

6 Structure-preserving discretization in time

In this section we comment on the time integration method applied to the constrained mechanical systems at hand. The specific structure-preserving scheme is second-order accurate and relies on previous works by Betsch & Steinmann [20] and Gonzalez [21]. If the underlying mechanical system is conservative, the present integrator conserves the total energy of the system. In addition to that, if the systems has symmetry, the present scheme conserves the associated momentum map. We won't dwell on the algorithmic conservation properties in the present work. Instead, we focus on the implications of natural coorinates for the numerical time integration.

Consider a representative time interval $[t_n, t_{n+1}]$ with time step $\Delta t = t_{n+1} - t_n$, and given state-space coordinates $\boldsymbol{q}_n \in \mathrm{Q}$ and $\boldsymbol{v}_n \in \mathbb{R}^n$ at time t_n. Concerning the initial values at t_0 we assume $\boldsymbol{q}_0 \in \mathrm{Q}$ and $\boldsymbol{v}_0 \in T_q\mathrm{Q}$. The resulting algebraic problem to be solved is stated as follows: Find $(\boldsymbol{q}_{n+1}, \boldsymbol{v}_{n+1}) \in \mathbb{R}^n \times \mathbb{R}^n$ and $\boldsymbol{\lambda}_{n,n+1} \in \mathbb{R}^m$ as the solution of the algebraic system of equations

$$\begin{aligned}
\boldsymbol{q}_{a_{n+1}} - \boldsymbol{q}_{a_n} &= \frac{\Delta t}{2}\left(\boldsymbol{v}_{a_n} + \boldsymbol{v}_{a_{n+1}}\right) \\
\sum_{b=1}^{\mathcal{N}} M^{ab}\left(\boldsymbol{v}_{b_{n+1}} - \boldsymbol{v}_{b_n}\right) &= \Delta t\left(\boldsymbol{F}^a_{n+\frac{1}{2}} - \overline{\nabla}_{\boldsymbol{q}_a} V_\lambda(\boldsymbol{q}_n, \boldsymbol{q}_{n+1})\right) \\
\boldsymbol{g}(\boldsymbol{q}_{n+1}) &= \boldsymbol{0}
\end{aligned} \tag{57}$$

for $a = 1, \ldots, \mathcal{N}$. In (57), $\overline{\nabla}_{\boldsymbol{q}_a} V_\lambda(\boldsymbol{q}_n, \boldsymbol{q}_{n+1})$ denotes a discrete derivative of the augmented potential function $V_\lambda : \mathbb{R}^n \mapsto \mathbb{R}$ in the sense of Gonzalez [22].

6.1 Rigid body constraints

Concerning the rigid body constraints dealt with in Section 3.1, we choose

$$\begin{aligned}
c_1 = c_2 = c_3 = 1 \\
c_4 = c_5 = c_6 = 0
\end{aligned} \tag{58}$$

In the continuous setting this choice of parameters is equivalent to the orthonormality of the director triad $\{\boldsymbol{d}_i(t)\}$ at all times. That is, in the continuos setting, $\boldsymbol{d}_i(t) \cdot \boldsymbol{d}_j(t) = \delta_{ij}$. However, using the mid-point approximation

$$\boldsymbol{d}_{i_{n+\frac{1}{2}}} = \frac{1}{2}\left(\boldsymbol{d}_{i_n} + \boldsymbol{d}_{i_{n+1}}\right) \tag{59}$$

in general destroys the orthonormality property, although it is still satisfied at the discrete times t_n and t_{n+1} due to $(57)_3$. That is,

$$\boldsymbol{d}_{i_{n+\frac{1}{2}}} \cdot \boldsymbol{d}_{i_{n+\frac{1}{2}}} \neq \delta_{ij} \tag{60}$$

This implies that the mid-point directors represent base vectors that in general are not of unit length nor mutually orthogonal.

6.2 Consistent application of external torques

Since the rigid body formulation described in Section 3 relies on skew coordinates, property (60) does not cause any difficulties. In particular, it is obvious from (41), that the director forces due to an external torque which enter the external force vector $\boldsymbol{F}^a_{n+\frac{1}{2}}$ in $(57)_2$ are given by

$$\boldsymbol{f}^i_{n+\frac{1}{2}} = \frac{1}{2}\boldsymbol{m}_{n+\frac{1}{2}} \times \boldsymbol{d}^i_{n+\frac{1}{2}} \tag{61}$$

Here, $\boldsymbol{m}_{n+\frac{1}{2}}$ represents an external torque applied in the time interval $[t_n, t_{n+1}]$, and $\boldsymbol{d}^i_{n+\frac{1}{2}}$ are contravariant mid-point directors that can be calculated from (9) such that property

$$\boldsymbol{d}^i_{n+\frac{1}{2}} \cdot \boldsymbol{d}_{j_{n+\frac{1}{2}}} = \delta^i_j \tag{62}$$

holds. It can be easily verified that the discrete balance of angular momentum can be written as

$$\boldsymbol{J}_{n+1} - \boldsymbol{J}_n = \Delta t \sum_{a=1}^{\mathcal{N}} \boldsymbol{q}_{a_{n+\frac{1}{2}}} \times \left(\boldsymbol{F}^a_{n+\frac{1}{2}} - \overline{\nabla}_{\boldsymbol{q}_a} V_\lambda(\boldsymbol{q}_n, \boldsymbol{q}_{n+1}) \right) \tag{63}$$

Note that the last equation can be viewed as discrete counterpart of the continuous version (56). If only one single rigid body is considered, (63) can be regarded as discrete counterpart of (31), where (3) has to be taken into account. Focusing on the contribution of the director forces (61) due to an external torque, for one single rigid body (63) yields

$$\begin{aligned}
\boldsymbol{J}_{n+1} - \boldsymbol{J}_n &= \Delta t \sum_{a=1}^{4} \boldsymbol{q}_{a_{n+\frac{1}{2}}} \times \boldsymbol{F}^a_{n+\frac{1}{2}} \\
&= \Delta t \boldsymbol{d}_{i_{n+\frac{1}{2}}} \times \boldsymbol{f}^i_{n+\frac{1}{2}} \\
&= \frac{\Delta t}{2} \boldsymbol{d}_{i_{n+\frac{1}{2}}} \times \left(\boldsymbol{m}_{n+\frac{1}{2}} \times \boldsymbol{d}^i_{n+\frac{1}{2}} \right) \\
&= \Delta t \left((\boldsymbol{d}_{i_{n+\frac{1}{2}}} \cdot \boldsymbol{d}^i_{n+\frac{1}{2}}) \boldsymbol{m}_{n+\frac{1}{2}} - (\boldsymbol{d}_{i_{n+\frac{1}{2}}} \cdot \boldsymbol{m}_{n+\frac{1}{2}}) \boldsymbol{d}^i_{n+\frac{1}{2}} \right) \\
&= \Delta t \boldsymbol{m}_{n+\frac{1}{2}}
\end{aligned} \tag{64}$$

Consequently, formula (61) guarantees that external torques are properly applied in the discrete setting. Formula (61) has originally been proposed in Betsch et al. [23]. However this work does not rely on skew coordinates for the description of rigid bodies. Contravariant mid-point directors have been introduced in [23, Sec. 4.3] to remedy the lack of angular momentum consistency in the discrete setting.

7 Inclusion of large deformation contact

The present framework for flexible multibody dynamics accomodates contemporary nonlinear finite elements and thus can be directly applied to large-deformation contact problems. In particular, unilateral contact constraints can be formulated as a set of inequality constraints which can be rewritten as equality constraints using a standard active set strategy. The node-to-surface (NTS) method (see Hesch & Betsch [18] for details) can be considered the prevailing method for contact problems in the context of finite elements. Actual developments extend the collocation-type NTS method to a variationally consistent formulation known as mortar contact method (see Hesch & Betsch [7, 19]). For both methods, the classical Karush-Kuhn-Tucker conditions read

$$g^{con} \leq 0, \quad \lambda^{con} \geq 0, \quad g^{con}\lambda^{con} = 0 \tag{65}$$

which can be rewritten as

$$\tilde{g}^{con} = \lambda^{con} - \max\{0, \lambda^{con} - c g^{con}\}, \quad c > 0 \tag{66}$$

This formulation makes possible a very efficient computer implementation of the active set strategy. We refer to [7, 19] for a full account on the present formulation of large deformation contact problems.

8 Numerical examples

8.1 Spacecraft attitude maneuver

In the first numerical example we demonstrate the importance of formula (61) for the consistent application of external torques. To this end we apply the present approach to the control of spacecraft rotational maneuvers.

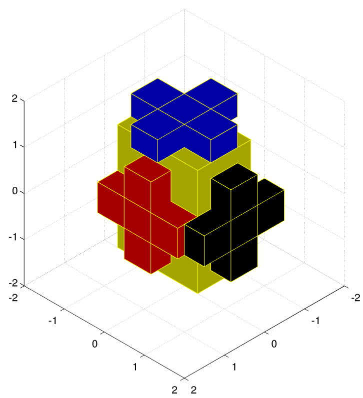

Figure 3: The spacecraft as 4-body system.

The spacecraft is modeled as multibody system consisting of four rigid bodies (Fig. 3), namely the base body and three reaction wheels. A similar example has been dealt with in Leyendecker et al. [24]. The data for the present 4-body system have been taken from [24]. Using principle axis for each rigid body the data used in the simulations are summarized in Table 1.

body	M_φ	E^{11}	E^{22}	E^{33}	L
1	1005.3096	89.3609	201.0619	357.4434	
2	424.1150	8.8357	106.0288	106.0288	0.9167
3	424.1150	106.0288	8.8357	106.0288	1.25
4	424.1150	106.0288	106.0288	8.8357	1.5833

Table 1: Spacecraft: Data for the 4-body system. Note that L denotes the distance between the center of mass of the reaction wheels and the base body.

The reaction wheels are spinning about body-fixed axis of the base body. For simplicity the three body-fixed axis are assumed to coincide with the director frame $\{{}^1\boldsymbol{d}_i\}$ of the base body. Spacecraft attitude maneuvers are performed by applying reaction wheel motor torques

$$ {}^2\boldsymbol{m} = (u^1)\,{}^1\boldsymbol{d}_1\,, \quad {}^3\boldsymbol{m} = (u^2)\,{}^1\boldsymbol{d}_2\,, \quad {}^4\boldsymbol{m} = (u^3)\,{}^1\boldsymbol{d}_3 \tag{67} $$

In the example we prescribe constant motor torques $u^i = 200$.

A total of $n = 48$ natural coordinates is employed to describe the multibody system at hand. Each body is subject to 6 rigid body constraints (22) and (58), giving rise to $m^{\text{int}} = 24$ internal constraints. Revolute joints are used to connect the reaction wheels to the base body. This amounts to $m^{\text{ext}} = 3 \times 5 = 15$ external constraints. Accordingly, in total there are $m = m^{\text{int}} + m^{\text{ext}} = 39$ independent constraints leading to $n - m = 9$ degrees of freedom.

The newly devised formula (61) has been used to consistently apply the motor torques to the reaction wheels. In this connection Remark 2.2 has been taken into account. That is, the torque acting on the base body is given by

$$ {}^1\boldsymbol{m} = -\left({}^2\boldsymbol{m} + {}^3\boldsymbol{m} + {}^4\boldsymbol{m}\right) \tag{68} $$

Since no resultant external torque acts on the spacecraft, the total angular momentum is a first integral of the motion. This can be verified along the lines of Section 6.2. In particular,

$$\begin{aligned}
\boldsymbol{J}_{n+1}-\boldsymbol{J}_n &= \Delta t \sum_{a=1}^{12} \boldsymbol{q}_{a_{n+\frac{1}{2}}} \times \boldsymbol{F}^a_{n+\frac{1}{2}} \\
&= \Delta t \sum_{b=1}^{4} {}^b\boldsymbol{d}_{i_{n+\frac{1}{2}}} \times {}^b\boldsymbol{f}^i_{n+\frac{1}{2}} \\
&= \frac{\Delta t}{2} \sum_{b=1}^{4} {}^b\boldsymbol{d}_{i_{n+\frac{1}{2}}} \times \left({}^b\boldsymbol{m}_{n+\frac{1}{2}} \times {}^b\boldsymbol{d}^i_{n+\frac{1}{2}}\right) \\
&= \Delta t \sum_{b=1}^{4} \left(({}^b\boldsymbol{d}_{i_{n+\frac{1}{2}}} \cdot {}^b\boldsymbol{d}^i_{n+\frac{1}{2}})\,{}^b\boldsymbol{m}_{n+\frac{1}{2}} - ({}^b\boldsymbol{d}_{i_{n+\frac{1}{2}}} \cdot {}^b\boldsymbol{m}_{n+\frac{1}{2}})\,{}^b\boldsymbol{d}^i_{n+\frac{1}{2}}\right) \\
&= \Delta t \sum_{b=1}^{4} {}^b\boldsymbol{m}_{n+\frac{1}{2}} \\
&= \boldsymbol{0}
\end{aligned} \tag{69}$$

In the numerical simulation we focus on the 3-component J_3 of the total angular momentum and the total kinetic energy T of the multibody system at hand. The numerical results due to the application of the newly devised formula (61) are denoted by J_3^{kontra} and T^{kontra}.

For comparison we apply the motor torques via the straightforward mid-point evaluation of the continuous expression of the 'original' formulation (see [23])

$$\boldsymbol{f}_{i_{n+\frac{1}{2}}} = \frac{1}{2}\boldsymbol{m}_{n+\frac{1}{2}} \times \boldsymbol{d}_{i_{n+\frac{1}{2}}} \tag{70}$$

The corresponding results are denoted by J_3^{kov} and T^{kov}.

A number of N time steps is used to resolve the time interval $[0,5]$. It can be observed from Fig. 4 that J_3^{kontra} stays constant for all N. This corroborates algorithmic conservation of the total angular momentum. In severe contrast to that J_3^{kov} does not stay constant. Accordingly the balance law for angular momentum is violated. This discretization error can be decreased by raising the number of time steps N. These observations are further supported by considering the total kinetic energy in Fig. 5. Accordingly, T^{kontra} does hardly change if the time steps are refined. That is, using only $N=5$ time steps already leads to a very good approximation of the kinetic energy. This is in severe contrast to T^{kov}.

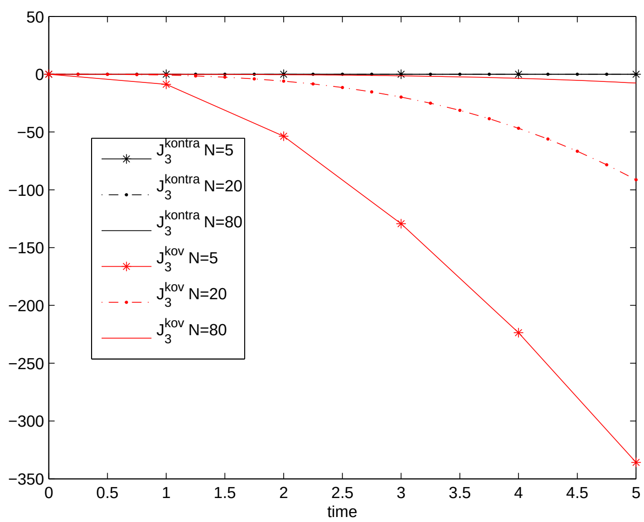

Figure 4: Spacecraft: Comparison of angular momentum.

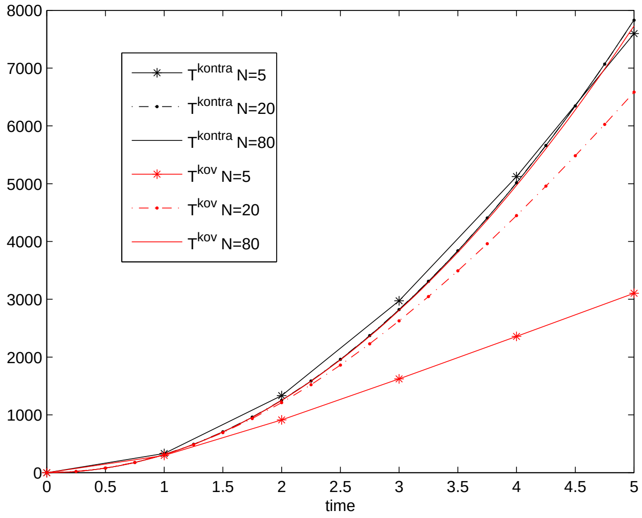

Figure 5: Spacecraft: Comparison of kinetic energy.

8.2 Lightweight robot applied to the mounting of flexible cables

The second example deals with a multibody model of the KUKA-DLR LightWeight Robot (LWR) (Bischoff et al. [25]) applied to the manipulation of highly flexible cables (Fig. 6). The LWR is modelled as multibody system with seven revolute joints. On the other hand the flexible cable is formulated as geometrically exact beam connected to a plug which itself is modelled as rigid body. The right end of the cable is clamped to a rigid block fixed in space.

In the forward simulation the end-effector grips the plug at the left end of the cable and subsequently bends the cable leading to large deformations. The joint-torques of the LWR are prescribed by applying the approach described in Section 6.2. Snapshots ot the motion are depicted in Fig. 7. In addition to that, in Fig. 8 the evolution of the total mechanical energy is shown along with the potential energy (due to gravity) and the strain energy stored in the cable.

i	a_i	α_i	d_i	θ_i
0	0	0	0	0
1	0	90	310	0
2	0	−90	0	0
3	0	−90	400	0
4	0	90	0	0
5	0	90	390	0
6	0	−90	0	0
7	0	0	0	0

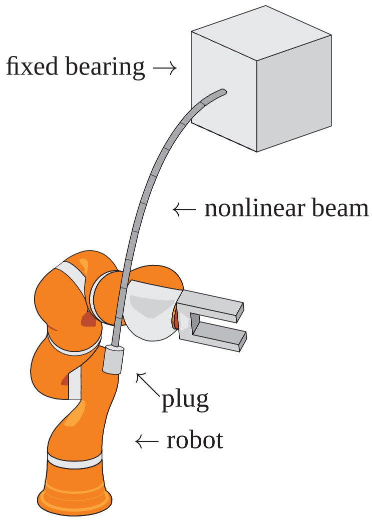

Figure 6: Hartenberg-Denavit parameters of the lightweight robot (left) and components of the flexible multibody system (right).

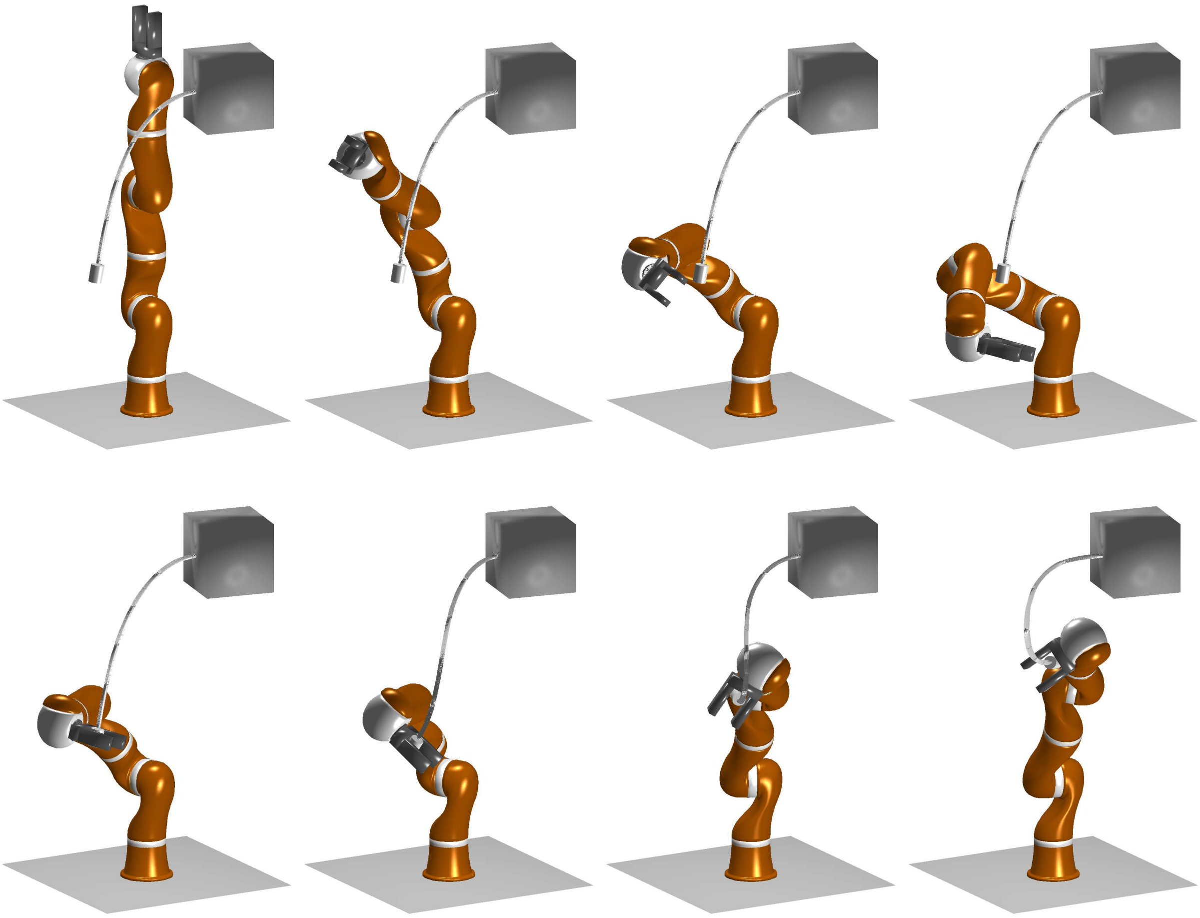

Figure 7: Snapshots of the motion for $t \in \{0, 1, 2, 5, 6, 7, 10, 12\}$.

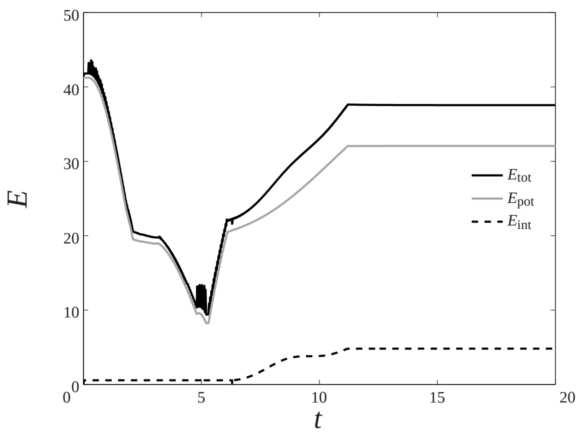

Figure 8: Energy evolution of the flexible multibody system: total energy E_{tot}, potential energy E_{pot} and internal strain energy E_{int}.

8.3 Tennis player

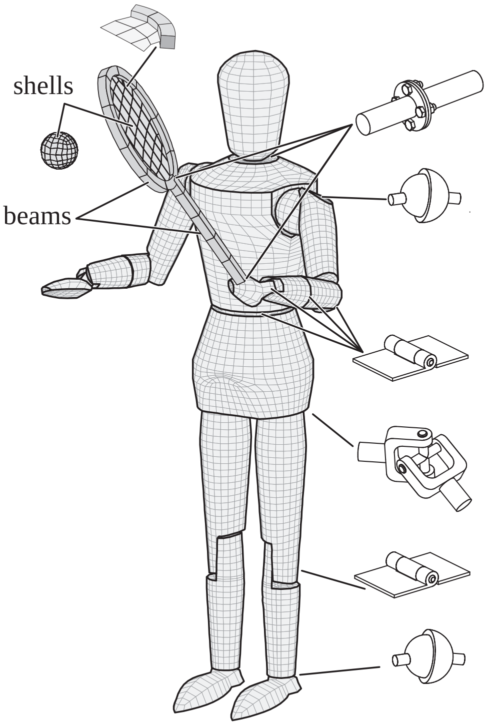

Figure 9: Multibody system with flexible components.

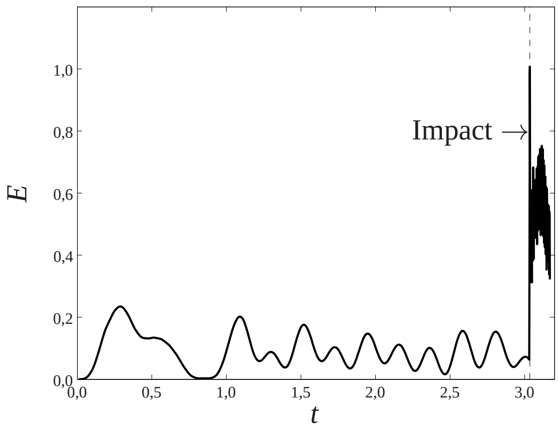

Figure 10: Strain energy of flexible components.

The last numerical example deals with the flexible multibody system depicted in Fig. 9. This example demonstrates the inclusion of geometrically exact beams and shells as well as large deformation contact within the present framework for flexible multibody dynamics. The model of a tennis player consists of 19 rigid bodies, whereas the tennis racket is modeled with nonlinear beams and shells (see Fig. 9). Shell elements are also used for modeling the tennis ball. The motion of the tennis player himself is prescribed (fully actuated). Due to the presence of the flexible tennis racket the whole system is highly underactuated. The motion of the system until the onset of contact between the tennis ball and the racket is illustrated with some snapshots in Fig. 11. The impact of the tennis ball on the racket leads to large deformations accompanied with a sudden increase of the strain energy (Fig. 10).

9 Conclusions

Natural coordinates allow for a systematic description of complex multibody systems. In this connection, the specific rigid body formulation described in Section 3 provides the link between standard multibody systems comprised of rigid bodies and flexible multibody systems resulting from the finite element discretization of deformable solids and structures. The present approach leads to a uniform set of differential-algebraic equations governing the motion of general flexible multibody systems. Moreover, the specific structure of the equations of motion makes possible the design of structure-preserving time-stepping schemes which exhibit superior numerical stability and robustness.

On the other hand, we have shown that the rigid body formulation in terms of natural coordinates requires particular caution when it comes to applying external torques. In a previous work (Betsch et al. [23]) an ad-hoc modification of the external forces has been proposed to restore the balance law for angular momentum in the discrete setting. In the present work this modification has been further substantiated by resorting to skew coordinates from the outset. It is worth noting that our approach has been guided by the theory of Cosserat points (Rubin [13]). It is obvious that the consistent formulation and numerical treatment of external torques is of crucial importance for the application of the present approach to the (optimal) control of (flexible) multibody systems.

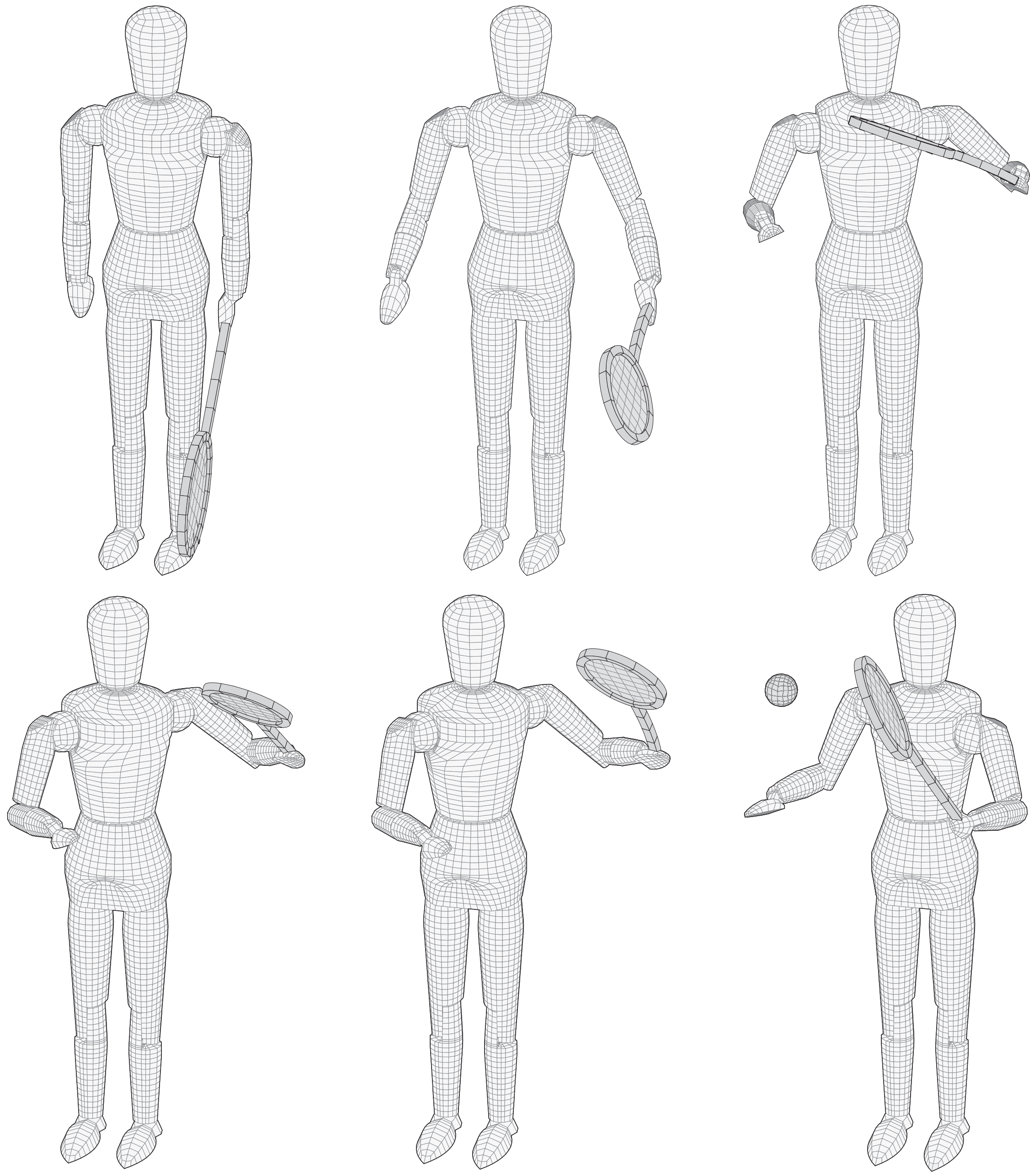

Figure 11: Snapshots of the motion.

Acknowledgment

Support for this research was provided by the Deutsche Forschungsgemeinschaft (DFG) under grant BE 2285/5. This support is gratefully acknowledged.

References

[1] P. Betsch and P. Steinmann. Constrained integration of rigid body dynamics. *Comput. Methods Appl. Mech. Engrg.*, 191:467–488, 2001.

[2] J. García de Jalón. Twenty-five years of natural coordinates. *Multibody System Dynamics*, 18(1):15–33, 2007.

[3] M. Groß and P. Betsch. Energy-momentum consistent finite element discretization of dynamic finite viscoelasticity. *Int. J. Numer. Meth. Engng*, 81(11):1341–1386, 2010.

[4] A. Ibrahimbegović and S. Mamouri. On rigid components and joint constraints in nonlinear dynamics of flexible multibody systems employing 3d geometrically exact beam model. *Comput. Methods Appl. Mech. Engrg.*, 188:805–831, 2000.

[5] P. Betsch and N. Sänger. On the use of geometrically exact shells in a conserving framework for flexible multibody dynamics. *Comput. Methods Appl. Mech. Engrg.*, 198:1609–1630, 2009.

[6] C. Hesch and P. Betsch. Transient three-dimensional domain decomposition problems: Frame-indifferent mortar constraints and conserving integration. *Int. J. Numer. Meth. Engng*, 82(3):329–358, 2010.

[7] C. Hesch and P. Betsch. A mortar method for energy-momentum conserving schemes in frictionless dynamic contact problems. *Int. J. Numer. Meth. Engng*, 77(10):1468–1500, 2009.

[8] A. Ibrahimbegović, S. Mamouri, R.L. Taylor, and A.J. Chen. Finite element method in dynamics of flexible multibody systems: Modeling of holonomic constraints and energy conserving integration schemes. *Multibody System Dynamics*, 4(2-3):195–223, 2000.

[9] S. Leyendecker, J.E. Marsden, and M. Ortiz. Variational integrators for constrained dynamical systems. *Z. Angew. Math. Mech. (ZAMM)*, 88(9):677–708, 2008.

[10] P. Betsch, C. Hesch, N. Sänger, and S. Uhlar. Variational integrators and energy-momentum schemes for flexible multibody dynamics. *J. Comput. Nonlinear Dynam.*, 5(3):031001/1–11, 2010.

[11] E.J. Saletan and A.H. Cromer. *Theoretical Mechanics*. John Wiley & Sons, 1971.

[12] S. Uhlar and P. Betsch. A rotationless formulation of multibody dynamics: Modeling of screw joints and incorporation of control constraints. *Multibody System Dynamics*, 22(1):69–95, 2009.

[13] M.B. Rubin. *Cosserat Theories: Shells, Rods and Points*, volume 79 of *Solid Mechanics and its Applications*. Kluwer Academic Publishers, 2000.

[14] J.E. Marsden and T.S. Ratiu. *Introduction to Mechanics and Symmetry*. Springer-Verlag, 2nd edition, 1999.

[15] P. Betsch and P. Steinmann. A DAE approach to flexible multibody dynamics. *Multibody System Dynamics*, 8:367–391, 2002.

[16] P. Betsch and P. Steinmann. Frame-indifferent beam finite elements based upon the geometrically exact beam theory. *Int. J. Numer. Meth. Engng*, 54:1775–1788, 2002.

[17] P. Betsch and P. Steinmann. Constrained dynamics of geometrically exact beams. *Computational Mechanics*, 31:49–59, 2003.

[18] C. Hesch and P. Betsch. Transient 3d contact problems–NTS method: mixed methods and conserving integration. *Computational Mechanics*, 48(4):437–449, 2011.

[19] C. Hesch and P. Betsch. Transient three-dimensional contact problems: mortar method. Mixed methods and conserving integration. *Computational Mechanics*, 48(4):461–475, 2011.

[20] P. Betsch and P. Steinmann. Conservation properties of a time FE method. Part III: Mechanical systems with holonomic constraints. *Int. J. Numer. Meth. Engng*, 53:2271–2304, 2002.

[21] O. Gonzalez. Mechanical systems subject to holonomic constraints: Differential-algebraic formulations and conservative integration. *Physica D*, 132:165–174, 1999.

[22] O. Gonzalez. Time integration and discrete Hamiltonian systems. *J. Nonlinear Sci.*, 6:449–467, 1996.

[23] P. Betsch, R. Siebert, and N. Sänger. Natural coordinates in the optimal control of multibody systems. *J. Comput. Nonlinear Dynam.*, 7(1):011009/1–8, 2011.

[24] S. Leyendecker, S. Ober-Blöbaum, J.E. Marsden, and M. Ortiz. Discrete mechanics and optimal control for constrained systems. *Optim. Control Appl. Meth.*, 31(6):505–528, 2010.

[25] R. Bischoff, J. Kurth, G. Schreiber, R. Koeppe, A. Albu-Schäffer, A. Beyer, O. Eiberger, S. Haddadin, A. Stemmer, G. Grunwald, and G. Hirzinger. The KUKA-DLR lightweight robot arm - a new reference platform for robotics research and manufacturing. *Robotics (ISR), 2010 41st International Symposium on and 2010 6th German Conference on Robotics (ROBOTIK)*, pages 1–8, 2010.